LASER WELDING IMPACT ON DEFORMATION PROPERTIES OF STEELS WHEN USED FOR CAR-BODY PARTS

EMIL EVIN[1], MIROSLAV TOMAS[2]

[1]Technical University of Kosice,
Faculty of Mechanical Engineering
Department of Automotive Production,
[2]Department of Computer Support of Technology,
Kosice, Slovak Republic

DOI: 10.17973/MMSJ.2016_11_2016112

e-mail: emil.evin@tuke.sk

The energy absorption at crash, usually described by stiffness and crashworthiness, is the key request for the car-body components, considering the material they were made from. The modified 3-point bending test with fixed ends has been developed in our department to assess materials for the car-body parts. The force and punch path are measured and used to calculate stiffness and crashworthiness. Experiments were performed on high strength low alloyed steel H220PD, dual phase steel DP 600 and austenitic stainless steels AISI 304 for base material and specimens welded by solid state fiber laser YLS-5000. Based on the experiments and analysis, the austenitic stainless steel is better to use for car body components of frontal deformation zones. Otherwise, the passenger's compartment is better protected by applying dual phase steel for car body parts when side impact occurs.

KEYWORDS
car-body, stiffness, crashworthiness, 3-point bending test, laser welding

1 INTRODUCTION

Recently, the pace of implementation of innovations in the automotive industry has been being increased. The innovations are oriented especially to meeting the safety requirements resulting from NCAP (New Car Assessment Programme) and from implementation of European legal regulations relating to the living environment, the so-called Kyoto Protocol. The intention of the NCAP project is to provide the customer with independent information on vehicle´s safety and to enable producers to obtain information on distinction of their automobiles from those of the competitors on the basis of frontal-impact, side-impact, pole-impact, and roof landing tests, and thus to increase competitiveness of their vehicles. [Vlk 2003, Wallentowitz 1996, Chvala 2005].

The „Euro NCAP" is the driving force for most of the automobile manufacturers engaged in development of active and passive elements of safety systems [Kramer 2009]. Passive safety elements do not include only internal safety (protection of passengers), but also external compatibility (aggressiveness rate to other traffic participants). In case of the external compatibility, it is about matching deformation forces and deformation travels, including distribution of the impact (absorbed) energy to the passengers involved in an accident, keeping biomechanical limit values, and maintaining the space for survival. Measures for ensuring internal and external safety serve for providing all traffic participants with the greatest hope for survival in case of an accident and for making the risk of injury as low as possible [Rediers 1998].

The forces are induced when the car impact occurs, including the deformation of each car body component. The factors such as vehicle speed and weight, structure stiffness, the deformation zones orientation and impact direction influence the extent of the car body damage. The car body deformation zones absorb the impact energy as well as provide the passengers safety when the accident occurs. The components of car body deformation zones are designed to deform in desired direction and absorb maximum energy as well. Thus, the destruction forces are decomposed and undesired impact energy must not penetrate the passenger's space [Vlk 2003].

Considering the safety, two basic requirements are laid to the deformation zones of the car body. The primary one is related to the front and rear parts of the car. These have to absorb maximum of deformation energy when frontal or rear impact occur. The basic requirement for the car body parts used in these areas is the high stiffness, good crashworthiness and high energy absorption level. The second requirement is focused to the well strength and stiffness of the car cabin for the passengers. The car cabin has to absorb maximum energy at small displacements or deflections of the components. So, the enough space for passengers surviving is secured when the accident occurs [Vlk 2003, Wallentowitz 1996].

Vehicle standards and regulations do not specify the design and materials of the components for the car body deformation zones. Thus, specified actions or safety characteristics have to be ensured when the impact occurs. However, rising requests to the safety characteristics increasing, the car weight and emissions reduction enforced the pressure to the evolution of new materials – high strength steels [Han 2016], aluminium alloys, plastics and composites – and unconventional production processes – laser welding of tailored blanks [Schrek 2016], hydro-mechanical forming, hydrofoming, hot metal gas forming, etc. Unconventional production processes of components used for passive safety components can influence the safety characteristics of these components when they are static or dynamic loaded [Chen 2015] by tension, compression, bending, torsion or shear, mainly compared to the conventional production processes.

Car body designers need information about both, safety characteristics of advanced materials and influence of the production process to these properties when design the car body structure. The safety characteristics of car body components are most often referred to the deformation work – toughness, strength, stiffness, fatigue etc. [Kramer 2009, Rediers 1998]

2 MATERIALS AND METHODS OF EXPERIMENT

The experimental research of the influence of the laser welding to the safety characteristics of car body components for deformation zones of car cabin have been performed using high strength low alloyed steel H220PD, dual phase steel DP 600 and austenitic stainless steels AISI 304. Measured values of mechanical properties and drawability properties measured in 90° to the rolling direction are shown in Tab. 1 and Tab. 2. Microstructure of base material is shown in Fig. 1.

Table 1. Mechanical properties of experimetal materials

Material	$R_{P0.2}$ [MPa]	Rm [Mpa]	Ag [%]	A_{80} [%]
H220PD	380	449	17	29
DP 600	376	632	19	28
AISI 304	302	765	58	62

Table 2. Deep-drawability parameters of experimental materials

Material	K [MPa]	n [-]	r [-]	ε_0 [%]
H220PD	728	0.178	0.659	37
DP 600	1096	0.217	0.766	12
AISI 304	1593	0.462	0.931	17

The metal steel blanks were laser welded in continual welding process with no gas using solid state fiber laser YLS-5000 by IPG laser. The metal steel blanks were clamped by table-clamps and stitched at the ends to prevent blanks deformation after weld metal solidification.

The material based approach to the assessment of weldability unalloyed, micro- and mid-alloyed steels is calculation of the carbon equivalent as follows:

$$C_E = C + \frac{Mn}{6} + \frac{Cr}{5} + \frac{Ni}{15} + \frac{Mo}{4} + \frac{Cu}{13} + \frac{P}{2} + 0.0024.a_0 \ [wgt\%] \quad (1)$$

and the Eq. (1) is valid for C <= 0.22 wgt. %, Mn <= 1.6 wgt. %, Cr <= 1 wgt. %, Ni <= 3 wgt. %, V <= 0.14 wgt %, Cu <= 0.30 wgt. % [2,4]. If $C_E \leq 0.5$ any special conditions are neccesary for welding. Considering the chemical composition of presented materials they meet this condition, so they weldability is guaranteed.

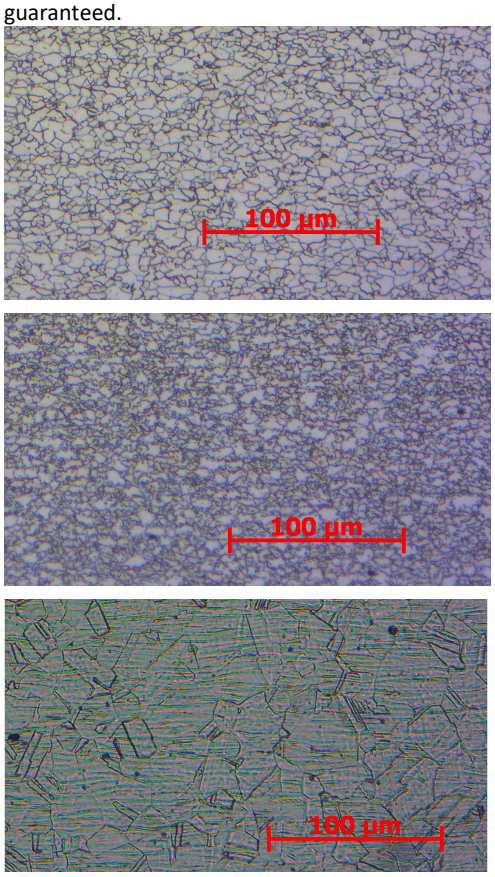

a) H220 PD

b) DP 600

c) AISI 304

Figure 1. Microstructure of base material

The optimisation of welding parameters – the welding speed and the power – has been realized by evaluation of macro and microstructures of welded joints – Fig. 2. The optimal ones for each material have been defined when any pores or cracks appeared in the weld material and good weld root quality was reached.

Samples in transversal direction for each welding mode applied have been taken in order to perform analysis of a weld joint macrostructure and microstructure of base material (BM), heat-affected zone (HAZ) and weld metal (WM). The visual inspection of the images of the microstructure and macrostructures did not detect pores and cracks in welds, and the weld roots were sufficiently penetrated. Thus it can be stated that:

a) out of the applied modes (welding speed of 50 mm.s^{-1} and the output of 2000 W, welding speed of 70 mm.s^{-1} and the output of 2700 W) of laser-beam welding of samples made of H220PD, the mode with the speed of 50 mm/s^{-1} and the output of 2000 W has been proved to be the most suitable,

b) out of the applied modes (welding speed of 50 mm.s^{-1} and the output of 1700 W, welding speed of 70 mm.s^{-1} and the output of 2100 W) of laser-beam welding of samples made of DP 600 and AISI 304, the mode with the speed of 50 mm.s^{-1} and the output of 1700 W has been proved to be the most suitable.

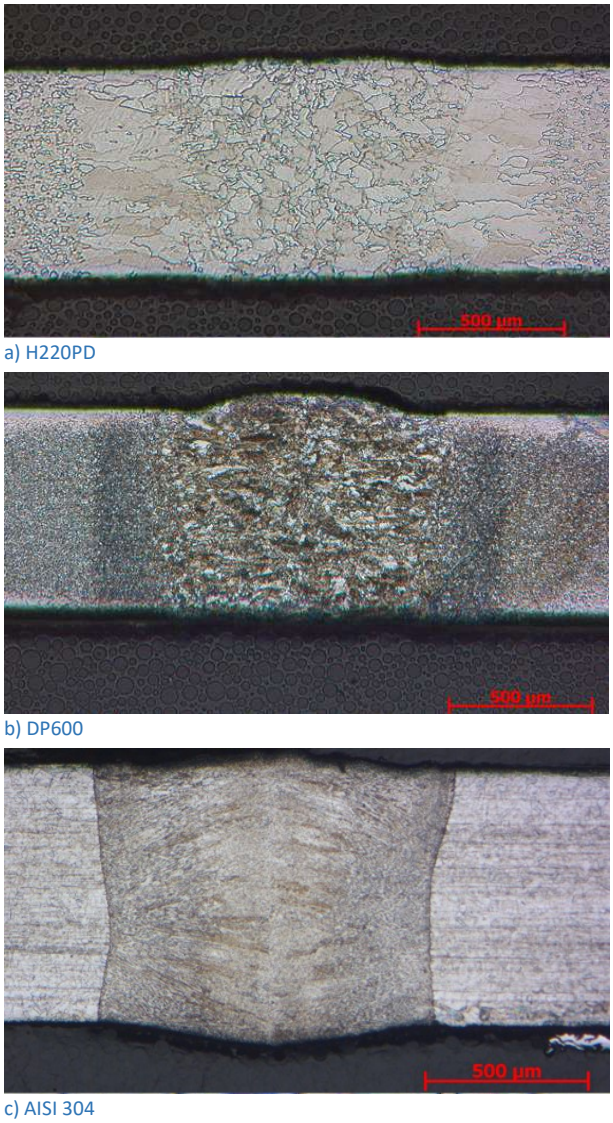

a) H220PD

b) DP600

c) AISI 304

Figure 2. Microstructure of laser weld joint

The safety characteristics were measured by modified 3-point bending test with fixed ends on the testing machine TIRAtest 2300. Non-standardized specimens of metal steel strips of 30 mm width and 300 mm length with and without the laser weld have been used. The thickness of metal steel strips was 0.75 mm for each material. The strips were laid at the cylinders of bending fixture and fasten by grips at the ends to prevent the strip pulling out – Fig. 3. The weld was oriented in longitudinal direction in the middle of the strip. The strip has been bending by punch until the strip fracture.

Figure 3. The bending fixture on the testing machine TIRAtest 2300

The bending force and the punch path have been recorded by PC during the test. The data have been saved in xls file and the deformation work, stiffness and deflection were calculated. Measured and calculated values are shown in Table 1. The main objective of the test was to find out the crack propagation – from the weld to the strip edge or from the strip edge to the weld – as well as compare the result for basic and welded materials. The distance of cylinders was 120 mm, the cylinder diameter 30 mm and the punch velocity 10 mm.min^{-1}.

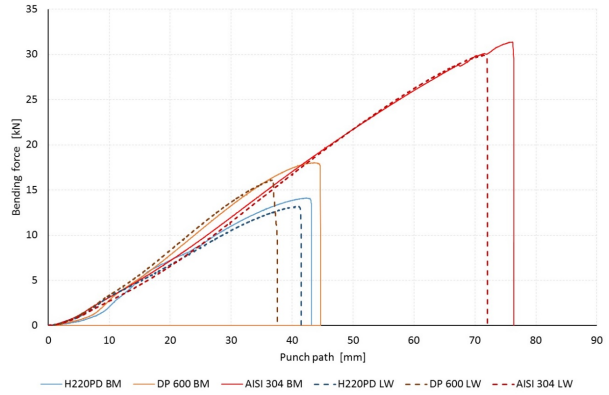

Figure 4. Bending force - punch path dependency experimentally measured for basic materials and laser-welded ones

The surface under the bending force-punch path curve when the maximum bending force is reached shows the deformation work of the material. The value has been calculated using curve's numerical integration by trapezoidal approximation of area under curve using Riemann's formula and its mid-point rule as follows:

$$W = \int_0^{h_{max}} F_B(h)dh \approx \sum_{i=1}^{n} F_{Bi}(\bar{h}_i)\Delta h = \Delta h\left[F_{B1}(\bar{h}_1) + F_{B2}(\bar{h}_2) + \ldots F_{Bn}(\bar{h}_n)\right] \quad (2)$$

where $\Delta h = h_{max}/n$, $\bar{h}_i$ is the center of interval $[h_{i-1}, h_i]$ and F_{Bi} is instantaneous bending force.

3 REACHED RESULTS AND DISCUSSION

Measured values of maximum bending force F_{Bmax} and total punch travel h_{max} are shown in Table 3. Calculated values of deformation work W_{pl} and stiffness constant c for each basic and welded material are shown in Table 4 and Table 5. These are compared in graphs for base material and laser welded one in Fig. 5, Fig. 6 and Fig. 7 respectively.

Table 3. Measured values of modified 3-point bending test

Material	Bending force F_{Bmax} [kN]		Deflection h_{max} [mm]	
	BM	LW	BM	LW
H220PD	14.3	13.2	43.2	41.5
DP 600	18.0	16.1	43.7	37.6
AISI 304	31.4	29.9	76.4	72.0

Table 4. Calculated values of deformation work

Material	Deformation work W_{pl} [Nm]			
	Deflection h_{max}		Deflection h = 30 mm	
	BM	LW	BM	LW
H220PD	320	307	163	164
DP 600	407	346	238	230
AISI 304	1245	1151	215	210

Table 5. Calculated values of stiffness constant

Material	Stiffness constant c [-]	
	BM	LW
H220PD	0.363	0.365
DP 600	0.528	0.510
AISI 304	0.467	0.478

Two basic concepts exist in the automotive industry for the car's safety: the first one is referred to the crashworthiness and the second one is referred to the penetration resistance of undesired fragments into the car cabin [Wallentowitz 1996]. The penetration resistance deals with energy absorption without penetration of projectile or fragment into the passenger's space, in combination with defined deformation of components or its defined displacement or deflection. The space between the passenger and car body is small – approx. 15 mm – when side impact occurs. Thus, components of deformation zone in this area have to absorb maximum impact energy at small displacement or deflection and it is expressed as follows: [Evin 2014, Evin 2013]

$$E_k = \frac{1}{2}mv_0^2 = \int_0^{\Delta x_{max}} F.dx \quad (3)$$

where m is the car weight, v_0 is the car velocity, dx is displacement or deflection of deformation zone components and F is deformation force.

As it is shown in Fig. 4 the bending force-punch path dependence is linear, so deformation force can be expressed as follows:

$$F_{max} = c.x_{max} \quad (4)$$

where c is the stiffness constant of the component and represents the stiffness of the component made out of given material and blank geometry, x_{max} is instant displacement or deflection when the force reaches the maximum value. Substituting the Eq. (4) to Eq. (3) and integration we get the equation for deformation work as follows:

$$W_{pl} = \frac{1}{2}mv_0^2 = \int_0^{\Delta x_{max}} c.x.dx = \frac{c.x^2}{2} \quad (5)$$

Stiffness constants c shown in Table 5 have been calculated by linear regression of bending force to punch path dependency within <15;75> % of the punch path (strip displacement or deflection) in order to eliminate instabilities at the test start.

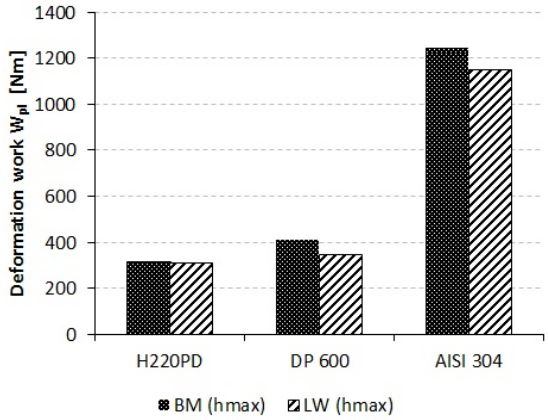

Figure 5. Deformation work for experimental materials when calculated for h_{max}

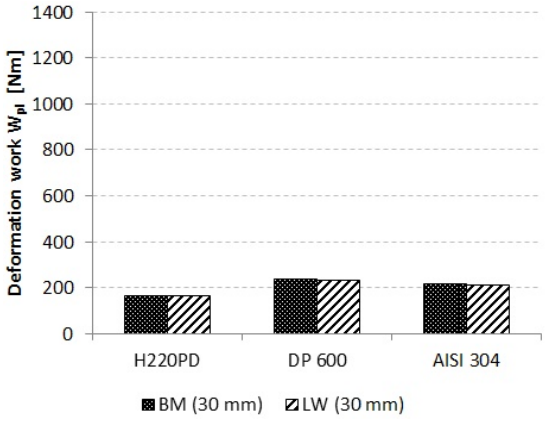

Figure 6. Deformation work for experimental materials when calculated for h = 30 mm

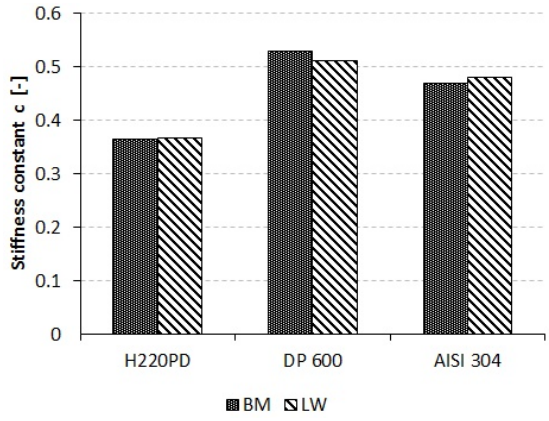

Figure 7. Stiffness constant comparison

The influence of laser welding have been found more intensively for multiphase materials – dual phase steel DP 600 (deformation work BM 407 Nm or LW 346 Nm – 15% lower) with ferrite-martensitic structure and austenitic stainless steel AISI 304 (BM 1245 Nm or LW 1151 Nm – 7.6 % lower) than for high strength low alloyed steel H220PD (BM 320 Nm or LW 307 Nm – 4.1 % lower). When consider the use of mentioned materials for deformation zones in the car doors area, the request of maximum displacement of 30 mm and minimal absorption energy of 200 Nm needs to be reached. In this case it is useful to meet the difference of total energy and energy when 30 mm displacement is reached should be as maximal possible.

If consider mentioned presumption, i.e. maximum displacement of 30 mm and minimal absorption energy of 200 Nm, then car body components made out of high strength low alloyed steel H220PD as well as laser welded did not meet these requirements, even the total deformation work was 320 Nm for BM and 307 Nm for LW. Thus, the total displacement of components would be larger than 300 mm. Car body components made out of dual phase steel DP600 and austenitic stainless steel AISI304 and its laser welded ones at 30 mm displacement are able to absorb the energy of 200 Nm and enough space of absorption ability is preserved as well. Even if the austenitic stainless steel AISI304 has the largest total deformation work, the dual phase steel DP 600 shows the higher reserve of absorption ability when consider the 30 mm displacement.

4 CONCLUSIONS

Based on the experimental research following outputs have been stated:

1. Materials used at experiments, high strength low alloyed steel H220PD, dual phase steel DP 600 and austenitic stainless steel AISI 304 have been welded without special conditions by laser welding. Macro and microscopic analysis have found no pores and cracks in weld metal and good quality of weld roots. Microstructure of base material H220PD is hypocutectoid ferrite and secondary intermixtures of carbides and nitrides. The structure of base material DP 600 is dual phase ferrite-martensitic with volume content of ferrite 70 % and martensite 30%. Microstructure of base material of austenitic steel AISI 304 is dendritic with austenitic matrices; delta ferrite arranged in rows as well as many globular carbide phases also have been found.

2. Researched materials have been welded by solid state fiber laser YLS-5000. Specimens were continuously welded with no protective gas and the velocity was 50 $mm.s^{-1}$ and 70 $mm.s^{-1}$. The optimal welding parameters have been found the velocity of 50 mm.s-1 for each material and the power of 2000 W when welding the high strength low alloyed steel H220PD and power of 1700 W when welding dual phase steel DP 600 and austenitic stainless steel AISI 304. Specimens have been welded without pre-heating and the cooling rate was approx. 1 s.

3. Microstructure of weld metal of high strength low alloyed steel H220PD is hypocutectoid ferrite and bainite. The structure of weld metal and heat affected zone of dual phase steel DP 600 is heterogenic with refined martensite in the heat affected zone and larger martensitic laths in the weld material. Microstructure of weld metal and heat affected zone of austenitic stainless steel AISI 304 is

austenitic with presence of delta ferrite mostly in grain boundaries. Microstructure is polyedric and the grain size reduces towards heat affected zone.

4. The highest deformation work shows the austenitic stainless steel AISI 304. However, dual phase steel DP 600 shows the higher reserve of deformation ability when consider 30 mm of displacement or deflection. The absorption ability of materials has been compared by deformation work at 30 mm of displacement or deflection. The higher values of absorption ability have been found for dual phase steel DP 600 and austenitic stainless steel AISI 304 than for high strength low alloyed steel H220PD.

ACKNOWLEDGMENTS

The paper has been worked out with the support of the grant project VEGA 2/0113/16 "Influence of laser welding parameters on structure and properties of welded joints of advanced steels for the automotive industry" and project APVV-0273-12 "Supporting innovations of autobody components from the steel sheet blanks oriented to the safety, the ecology and the car weight reduction".

REFERENCES

[Chen 2015] Chen H. et al. Vehicle front structure energy absorbing optimization in frontal impact. Open Mechanical Engineering Journal, 2015, Vol. 9 , Iss. 1, pp. 168-172. ISSN 1874-155X

[Chvala 2005] Chvala R. and Sperkova A. How Euro NCAP works. [online]. Bratislava, 2005 [cit. 2013-12-09]. Available from: <http://auto.sme.sk/c/2247701/ako-funguje-euro-ncap.html>

[Evin 2013] E. Evin et al. Design of dual phase high strength steel sheets for autobody. DAAAM International Scientific Book 2013. Vienna: DAAAM International, 2013, pp. 767-786. ISBN 978-3-901509-94-0

[Evin 2014] Evin E. et al. The Deformation Properties of High Strength Steel Sheets for Auto-Body Components. In: Procedia Engineering, 2014, Vol. 69, pp. 758-767. ISSN 1877-7058

[Han 2016] Han, Z. Y. et al. Research and application of high performance automobile steel. Iron and Steel, 2016, Vol. 51, Iss. 2, pp. 1-9.

[Kramer 2009] Kramer F. Passive Sicherheit von Kraftfahrzeugen. Weisbaden: Vieweg+Teubner, 2009. ISBN 978-3-8348-0536-2

[Rediers 1998] Rediers B. et al. Static and dynamic stiffness-One test both results. In: Proc. of the 16th IMAC, 1998, pp 30-35

[Schrek 2016] Schrek, A. et al. Deformation properties of tailor-welded blank made of dual phase steels. Acta Mechanica et Automatica, 2016, Vol. 10, Iss. 1, pp. 38-42. ISSN 1898-4088

[Vlk 2003] Vlk, F. Car-bodies of vehicles. 1st ed., Brno: Publishing Co. Vlk, 2003. ISBN 80-238-5277-9

[Wallentowitz 1996] Wallentowitz H. and Adam H. Predicting the crashworthiness of vehicle structures made by lightweight design materials and innovative joining methods. International Journal of Crashworthiness, 1996, Vol. 1, Iss. 2, pp 163-180. ISSN 1358-8265

CONTACTS:

prof. Ing. Emil Evin, CSc.
Technical University of Kosice
Faculty of Mechanical Engineering
Department of Automotive Production
Masiarska 74, 040 01 Kosice, Slovak Republic
Tel.: + 421 55 602 3547
e-mail: emil.evin@tuke.sk

Ing. Miroslav Tomas, Ph.D.
Technical University of Kosice
Faculty of Mechanical Engineering
Department of Computer Support of Technology
Masiarska 74, 040 01 Kosice, Slovak Republic
Tel.: + 421 55 602 3524
e-mail: miroslav.tomas@tuke.sk